Synthesis and characterization of new *N*-{4,6-bis[2-(het)arylvinyl]pyrimidin-2-yl}-substituted polycyclic aromatic imides

E. A. Komissarova,[a,b] A. N. Vasyanin,[b] V. E. Zhulanov,[b] I. V. Lunegov,[b] E. V. Shklyaeva,[b] and G. G. Abashev[a,b]★

[a] *Institute of Technical Chemistry, Ural Branch of the Russian Academy of Sciences, 3 ul. Akad. Koroleva, 614013 Perm, Russian Federation. Tel.:+7 (342) 237 8289. E-mail: gabashev@psu.ru*
[b] *Perm State University, 15 ul. Bukireva, 614990 Perm, Russian Federation. Tel.: +7 (342) 239 6231. E-mail: ekaterina.komva@gmail.com*

Two series of new *N*-{4,6-bis[2-(het)arylvinyl]pyrimidin-2-yl}-substituted aromatic polycyclic imides were synthesized. The synthesized chromophores were characterized by UV and fluorescence spectroscopy, cyclic voltammetry, and quantum chemical density functional theory calculations. A change in the nature of aryl (hetaryl) moieties was found to cause changes in the optical properties of both solutions of these compounds and thin films prepared from these compounds. The replacement of the phthalimide moiety by the 1,8-naphthalimide one has led to a significant increase in the lowest unoccupied molecular orbital energy.

Key words: phthalimide, 1,8-naphthalimide, pyrimidine, chromophore, quantum chemical calculations.

Pyrimidine is a highly π-deficient aromatic heterocycle and is often incorporated, as an efficient electron-withdrawing moiety, into small molecules, oligomers, and polymers behaving as push-pull chromophores.[1—6] A π-conjugated system composed of this moiety and electron-donating aromatic carbo- and heterocycles linked by a π-conjugated bridge causes an effective photoinduced intramolecular charge transfer in the compound, giving rise to fluorescence and nonlinear optical properties.

4,6-Bis[2-aryl(hetaryl)vinyl]-substituted pyrimidines have been extensively studied since the early 2000s. These compounds are described as pH sensors,[5,7,8] luminescent materials for organic light-emitting diodes,[9,10] and materials with nonlinear optical properties.[9,11] Pyrimidine derivatives are also used as semiconductor layers in organic field-effect transistors.[12—14]

2-Amino-4,6-dimethylpyrimidine is an important starting compound for the preparation of the extended π-conjugated systems exhibiting valuable properties, which are of interest for organic electronics. This compound contains reactive methyl groups, which can act as components in different condensation reactions,[7] and an amino group, which has both basic and nucleophilic properties and, as a consequence, is capable of being involved into the condensation reactions with aliphatic and aromatic aldehydes, diazotization,[15] alkylation,[16] and acylation.[17] Besides, acid anhydrides and, in particular, cyclic dicarboxylic acid anhydrides, are important acylating agents. The use of these compounds allows to synthesize such promising small molecules as electron-deficient *N*-substituted polycyclic imides. The latter compounds are utilized as semiconductor materials with electron conductivity and are employed in organic field-effect transistors.[18—20] Most of these polycyclic imides bear an alkyl substituent at the nitrogen atom, the presence of which increases solubility of the compounds and, consequently, improves their film-forming properties. Besides, the introduction of alkyl substituents leads to the improvement of conductivity because alkyl chains interact with each other, thereby bringing the molecules in close proximity and facilitating more efficient overlap of π-orbitals of conjugated moieties in the molecules.[18,19] *N*-Aryl- and *N*-hetaryl-substituted polycyclic imides are much less studied.[21—26] Under ambient conditions, *N*-aryl-substituted naphthalene-1,4,5,8-tetracarboxylic or perylene-3,4,9,10-tetracarboxylic acid diimides bearing 3-alkoxy-1-phenyl-1,2,3,4-tetrahydroquinoline moieties at the periphery were found to have both hole and electron conductivity at the ambient conditions.[27] The simultaneous presence of electron-donating (carbazole, thiophene, pyrrole) and electron-withdrawing (pyrimidine, phthalimide, 1,8-naphthalimide) moieties facilitates strong intramolecular charge transfer, which has a direct effect on optical and electrochemical properties. 1,8-Naphthalimides containing both the electron-withdrawing pyridine ring at the imide nitrogen atom and an electron-donating substituent at position 4 of the naphthalene ring exhibit interesting optical properties, in particular, tuning fluores-

Published in Russian in *Izvestiya Akademii Nauk. Seriya Khimicheskaya,* No. 9, pp. 1702—1713, September, 2019.
1066-5285/19/6809-1702

cence in different aggregated states.[28] Therefore, the synthesis of polycyclic imides containing different electron-donating carbo- and heterocyclic moieties are of obvious interest.

Previously, we synthesized and characterized symmetrical and unsymmetrical 4,6-bis[2-(het)arylvinyl]-pyrimidines bearing electron-donating alkoxy- and alkylmercapto substituents at position 2 of the pyrimidine ring.[29—32] The goal of this work is to synthesize Y-shaped D—π-A—π-D-type chromophores, which contain aromatic imide (phthalimide or 1,8-naphthalimide) attached through its nitrogen atom to atom C(2) of the pyrimidine ring as the electron-withdrawing core, investigate the optical and electrochemical properties of the synthesized compounds, and determine the energy characteristics of the molecules by experimental methods and quantum chemical calculations.

Results and Discussion

The target compounds were synthesized as follows. First, the main starting compound, *viz.*, 2-amino-4,6-dimethylpyrimidine (**1**), was prepared by the cyclocondensation of acetylacetone with urea.[33] 9-Hexyl-9*H*-carbazole-3-carbaldehyde was synthesized by the Vilsmeier—Haack reaction from 9-hexyl-9*H*-carbazole, which was prepared by the alkylation of carbazole with 1-bromohexane in DMF in the presence of NaOH.[34] The heating of 2-amino-4,6-dimethylpyrimidine **1** with phthalic and 1,8-naphthalic anhydrides at reflux in anhydrous DMF under an argon atmosphere afforded 2-(4,6-dimethylpyrimidin-2-yl)phthalimide (**2**) described earlier[26] and 2-(4,6-dimethylpyrimidin-2-yl)-1,8-naphthalimide (**3**) (Scheme 1). Previously, 2-(4,6-dimethylpyrimidin-2-yl) phthalimide (also referred to as 2-(4,6-dimethylpyrimidin-2-yl)isoindoline-1,3-dione) was synthesized by heating the same starting compounds at reflux in a minimum amount of toluene at 200 °C.[26]

The condensation of *N*-acylated 4,6-dimethylpyrimidines **2** and **3** with appropriate carbaldehydes in a 5 *M* aqueous NaOH solution in the presence of the phase-transfer catalyst Aliquat 336[35] gave target conjugated pyrimidines **4**—**11** (see Scheme 1). These compounds are D—π-A—π-D-type chromophores containing a combination of pyrimidine and aromatic imide moieties linked together through the imide nitrogen atom, as the electron-withdrawing core.

All Y-shaped pyrimidines **2**—**11** were synthesized in high yields (68—85%) and were isolated and purified by silica gel column chromatography. The structures of all

Scheme 1

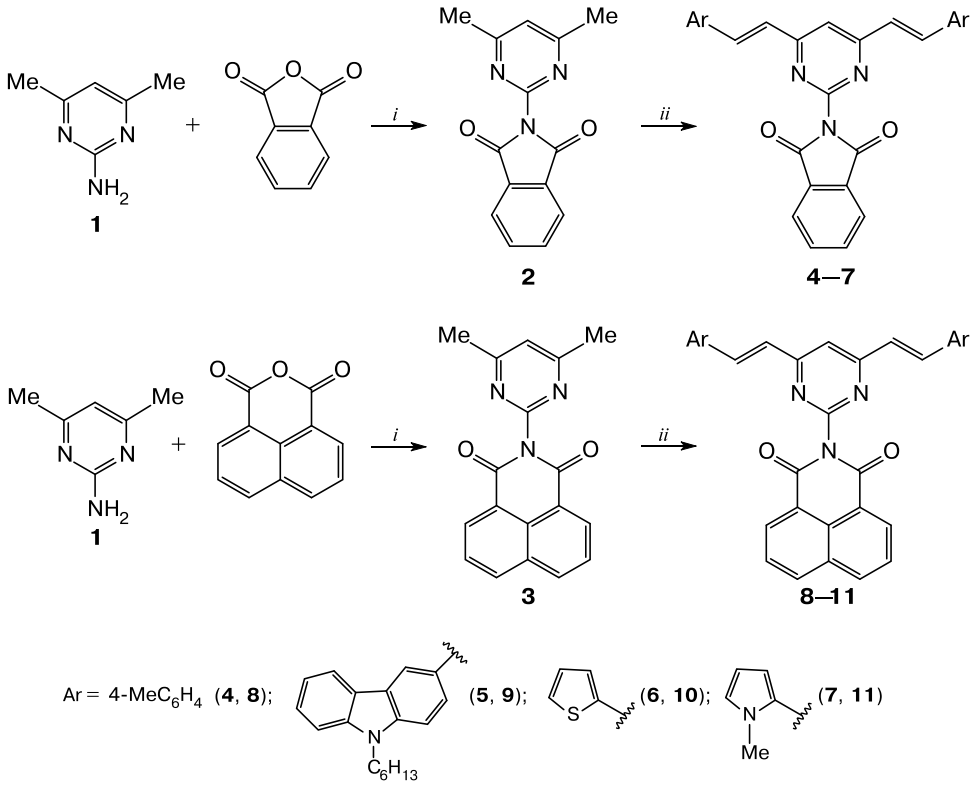

Reagents and conditions: *i*. DMF, reflux, 24 h, argon atmosphere; *ii*. ArCHO, Aliquat 336, 5 *M* NaOH, reflux, 5 h, argon atmosphere.

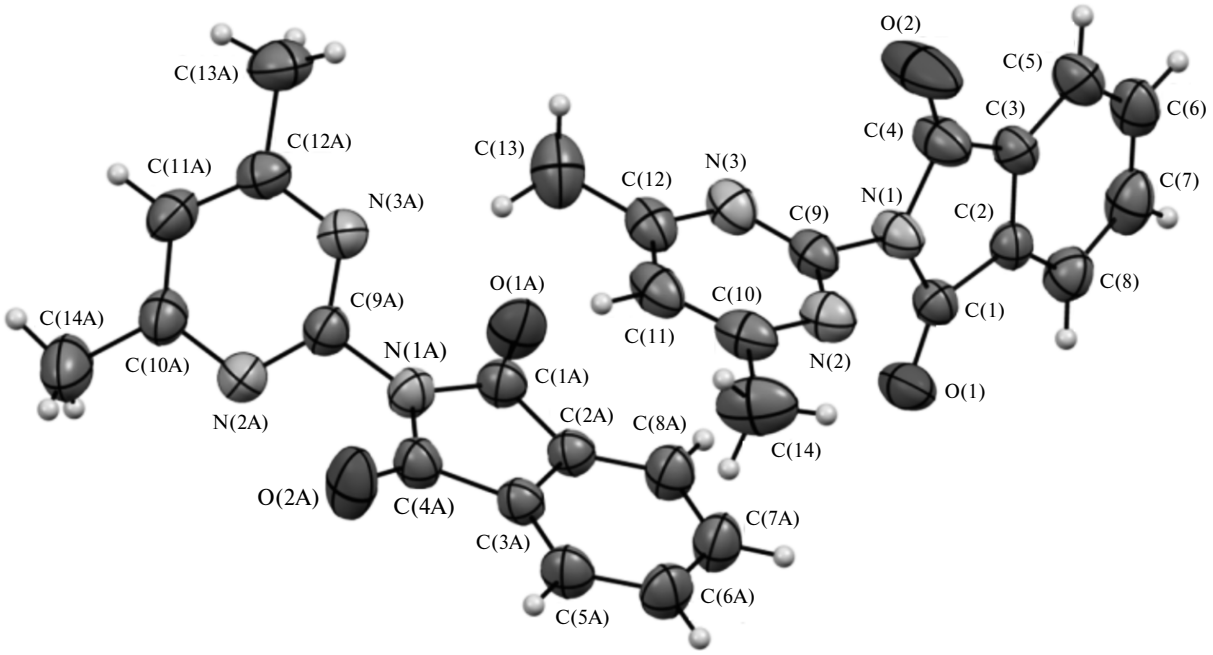

Fig. 1. Crystal structure of compound **2** (CCDC 1883703) with thermal ellipsoids drawn at the 50% probability level.

compounds were confirmed by ^{1}H and ^{13}C NMR spectroscopy and elemental analysis. Chromophores **2**—**11** are readily soluble in common organic solvents. For chromophores **2** and **3**, we obtained crystals suitable for X-ray diffraction. Compounds **2** and **3** have the same molecular geometry. Compound **2** crystallizes in the centrosymmetric triclinic space group. There are two crystallographically independent molecules of compound **2** with similar geometry per asymmetric unit (Fig. 1). All bond lengths and most bond angles fall within the normal ranges indicated by Mercury Mogul Geometry Check.[36] The pyrimidine and phthalimide moieties in compounds **2** and **3** are planar within ~0.002 Å. The dihedral angles between the planes of the pyrimidine and phthalimide moieties of two independent molecules are 57.9 and 69.5°. The crystal packing of compound **2** is shown in Figs 2 and 3. It can be seen that there is π—π conjugation between the pyrimidine rings. The distances between the centroids of the phthalimide moieties of two identical molecules are 3.71 and 4.08 Å; the distances between the planes of two phthalimide moieties are 3.51 and 3.85 Å, respectively (see Fig. 3). The distance between phthalimide moiety and the aromatic ring of the imide moiety of two independent molecules is 3.95 Å. The distances between the centroids of two aromatic rings of the imide moieties of the identical molecules are 3.89 and 6.65 Å; the distances between the planes of two imide moieties are 3.58 and 3.28 Å (see Fig. 2).

Compound **3** crystallizes in the centrosymmetric monoclinic space group. There are two crystallographically independent molecules of compound **3** with similar geometry per asymmetric unit (Fig. 4). The 1,8-naphthalimide moiety and the pyrimidine ring are planar within 0.006 and 0.003 Å, respectively. The dihedral angles between the planes of the 1,8-naphthalimide moiety and the pyrimidine ring in two independent molecules are 78.0 and 82.8°. The crystal packing of compound **3** is shown in Fig. 5. In the crystal, the molecules are arranged in an antiparallel fashion. The π—π interaction between the antiparallel layers is observed at a distance of 3.59 Å. The planes of the 1,8-naphthalimide moieties of two crystal-

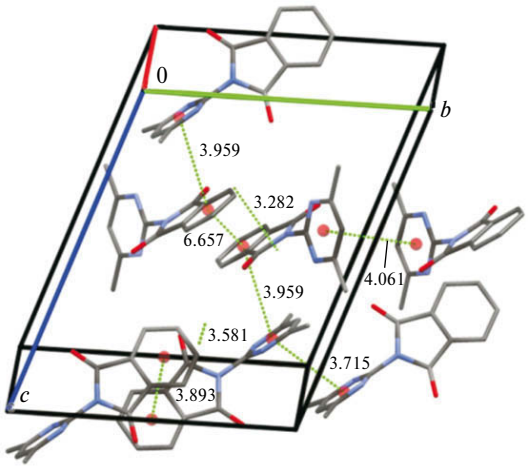

Fig. 2. Single crystal unit cell of compound **2** (general view). *Note*. Figures 2, 3, 5, 6, and 9 are available in full color on the web page of the journal (https://link.springer.com/journal/volumesAndIssues/11172).

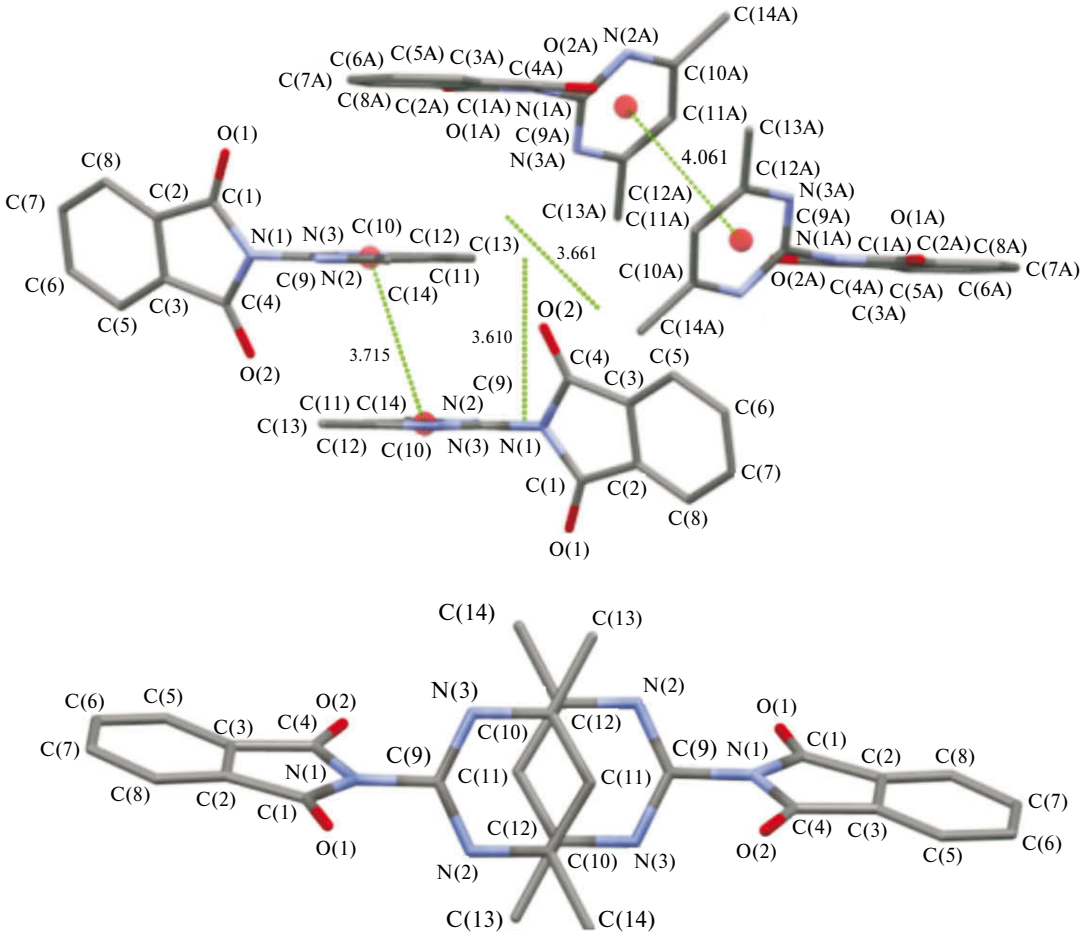

Fig. 3. Single crystal unit cell of compound **2** (detailed arrangement).

lographically independent molecules are inclined with respect to each other by an angle of 5.5°. The distance between the centroid of the 1,8-naphthalimide moiety of one independent molecule and the plane of the pyridine ring of another independent molecule is 3.66 Å.

Cyclic voltammetry (CV) was used to study the electrochemical behavior of the synthesized compounds and evaluate the frontier orbital energies. The cyclic voltammograms of the compounds containing the phthalimide moiety (**2**, **4**—**7**) show three reduction peaks (E_{red}) at

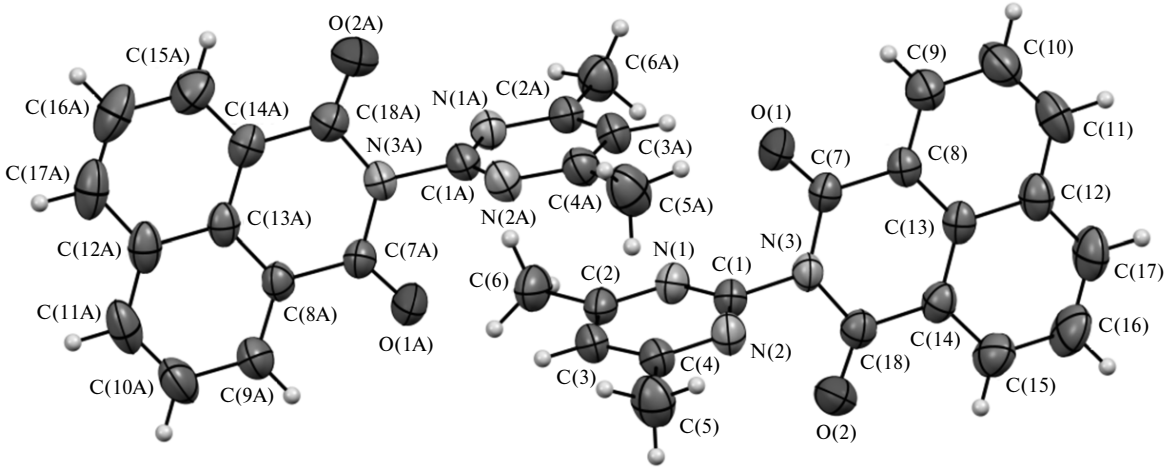

Fig. 4. Molecular structure of compound **3** (CCDC 1883705) with thermal ellipsoids drawn at the 50% probability level.

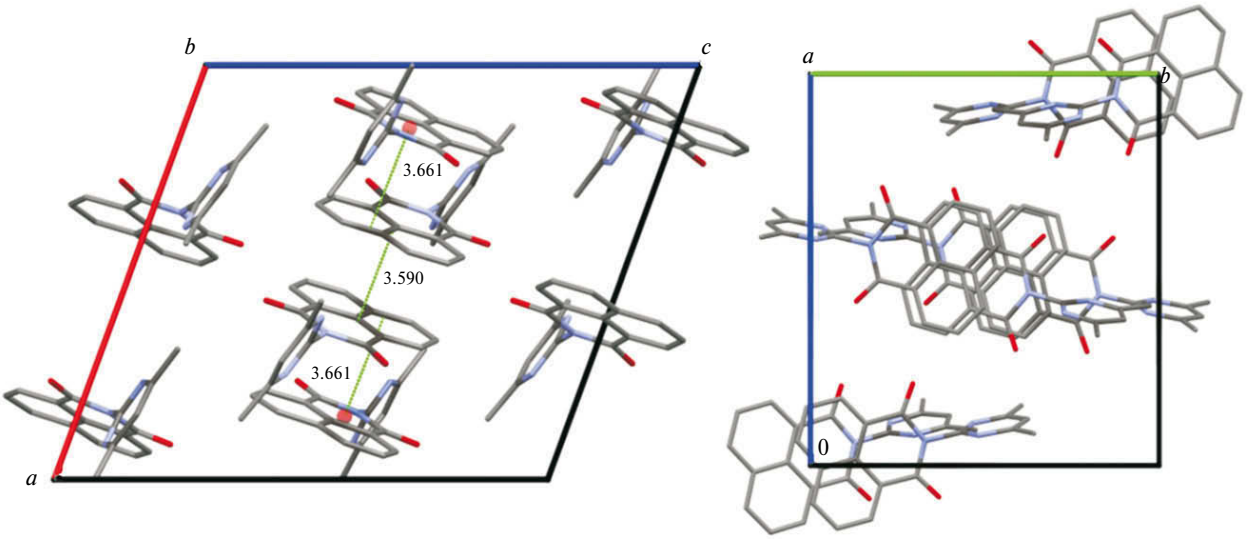

Fig. 5. Single crystal unit cell of compound **3**.

–0.86, –1.31, and –1.62 V (Fig. 6). The oxidation peaks in the CV curves of compounds **4**—**7** are assigned to anodic oxidation of electron-donating (thiophene, *N*-methylpyrrole, *N*-hexylcarbazole, and *p*-tolyl) moieties of the molecules resulting in dimers formation. The cyclic voltammograms of almost all compounds bearing the 1,8-naphthalimide moiety (**8**—**11**), except for compound **3**, show one broadened reduction peak at –1.6 V. The oxidation peaks (E_{ox}) also correspond to oxidation of electron-donating moieties of the molecules (Fig. 7).

Substituted aromatic imides are used for the design of materials with electron conductivity. It is generally assumed that stable electron injection, high charge carrier mobility, and resistance of organic semiconductors to air oxidation require that the lowest unoccupied molecular orbital (LUMO) energy is smaller than or equal to –4.0 eV. The values of the E_{LUMO} falling in the interval from –4.3 to –4.4 eV are treated to be the most preferable.[18,37] To achieve this electron affinity, electron-withdrawing groups should be introduced into the structure of the expected

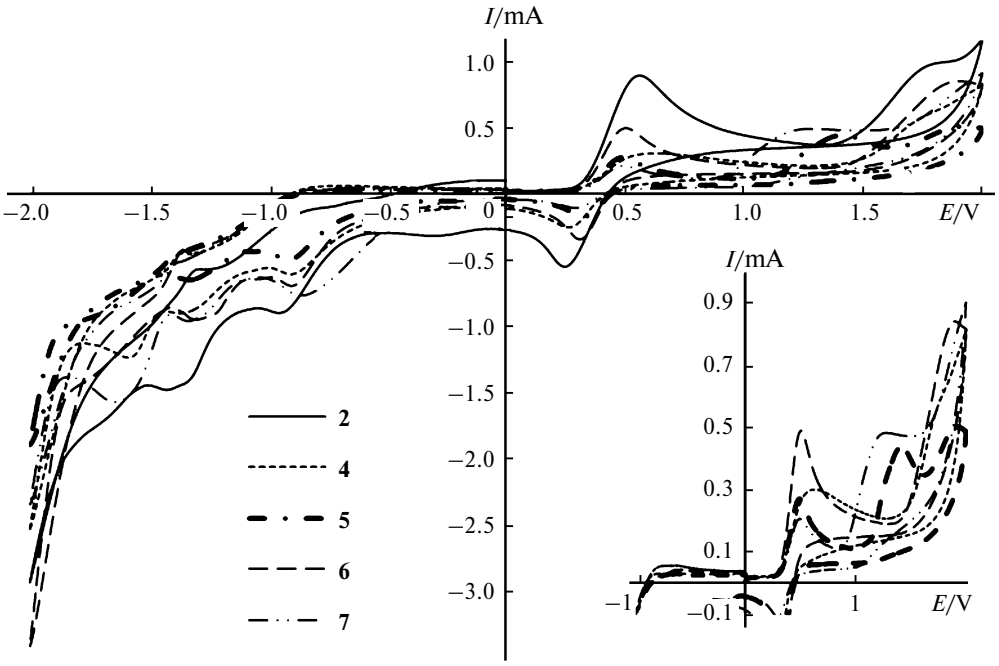

Fig. 6. CV curves of pyrimidines **2** and **4**—**7**.

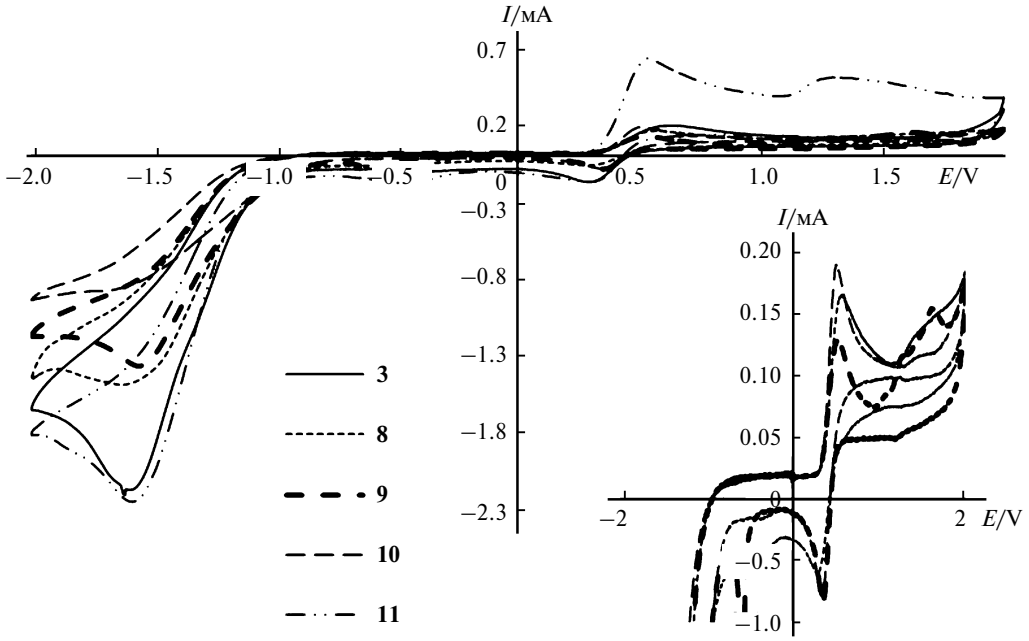

Fig. 7. CV curves of pyrimidines **3** and **8**—**11**.

semiconductor as substituents at nitrogen or carbon atoms in the aromatic core of polycyclic imide. The embedding of the pyrimidine ring into the structure of any conjugated molecule generally leads to a decrease in the LUMO energy, which, in turn, facilitates high electron mobility. For the synthesized pyrimidines, the highest occupied molecular orbital (HOMO) and LUMO energies for compounds **2** and **3** are −6.22/−4.16 eV and −6.45/−3.77 eV, respectively (Table 1). An increase in the conjugation length of chromophores **4**—**11** by introducing 2-aryl-(hetaryl)vinyl substituents at positions 4 and 6 of the pyrimidine ring leads to a change in the energy characteristics of the molecules, in particular, to a decrease in the band gap width. The presence of both phthalimide and 1,8-naphthalimide moieties leads to an increase in the ionization potential (E_{HOMO}) for the carbazole- and pyrrole-containing chromophores (**5**, **7**, **9**, **11**), the LUMO energy being decreased. This also causes a decrease in the band gap width (E_g^{elc}), particularly in compounds **5**, **7**, and **9** (see Table 1). The highest occupied molecular orbital energy (E_{HOMO}) for compounds **5**, **7**, **9**, and **11** varies from −5.92 to −5.72 eV. The HOMO energies (E_{HOMO}) of tolyl- and thiophene-substituted *N*-pyrimidin-2-ylphthalimides **4** and **6** are −6.23 and −6.25 eV, respectively, which are only slightly lower than the corresponding value determined for the starting 4,6-dimethylpyrimidin-2-ylphthalimide **2** (−6.22 eV). The average electron affinity (also referred to as E_{LUMO}) for 4,6-disubstituted pyrimidin-2-yl-1,8-naphthalimides **8**—**11** is −3.9 eV; for related compounds **4**—**7** bearing the phthalimide moiety, this parameter is in the range from −4.38 to −4.23 eV.

Therefore, the LUMO level of the target products can be tuned by changing the nature of the substituent at position 2 of the pyrimidine ring. The LUMO energy for 4,6-disubstituted pyrimidin-2-yl-1,8-naphthalimides **8**—**11** is in the range from −3.98 to −3.80 eV; for 4,6-disubstituted pyrimidin-2-yl-phthalimides **4**—**7**, the LUMO energy ranges from −4.38 to −4.23 eV (see Table 1). These

Table 1. The HOMO/LUMO energies and band gaps (E_g^{elc}) of compounds **2**—**11**, which were experimentally determined (I) and calculated (II)

Compound	I[a]			II[b]		
	E_{HOMO}	E_{LUMO}	E_g^{elc}	E_{HOMO}	E_{LUMO}	E_g^{elc}
	eV					
2	−6.22	−4.16	2.06	−7.43	−2.20	5.26
3	−6.45	−3.77	2.68	−6.91	−2.48	4.42
4	−6.23	−4.27	1.96	−6.23	−2.24	3.99
5	−5.92	−4.28	1.64	−5.86	−2.25	3.61
6	−6.25	−4.23	2.02	−6.18	−2.40	3.78
7	−5.72	−4.38	1.34	−5.56	−2.17	3.39
8	−6.03	−3.92	2.11	−6.20	−2.41	3.79
9	−5.81	−3.95	1.86	−5.85	−2.45	3.39
10	−6.10	−3.98	2.12	−6.16	−2.44	3.72
11	−5.92	−3.80	2.12	−5.54	−2.44	3.10

[a] The values were determined from the CV curves: $E_{HOMO}(eV) = -(E^{ox}_{onset\ vs\ Fc/Fc^+} + 4.80)$, $E_{LUMO}(eV) = -(E^{red}_{onset\ vs\ Fc/Fc+} + 4.80)$;[41,42] $E_g^{elc}(eV) = E_{HOMO} - E_{LUMO}$;
[b] quantum chemical calculations.

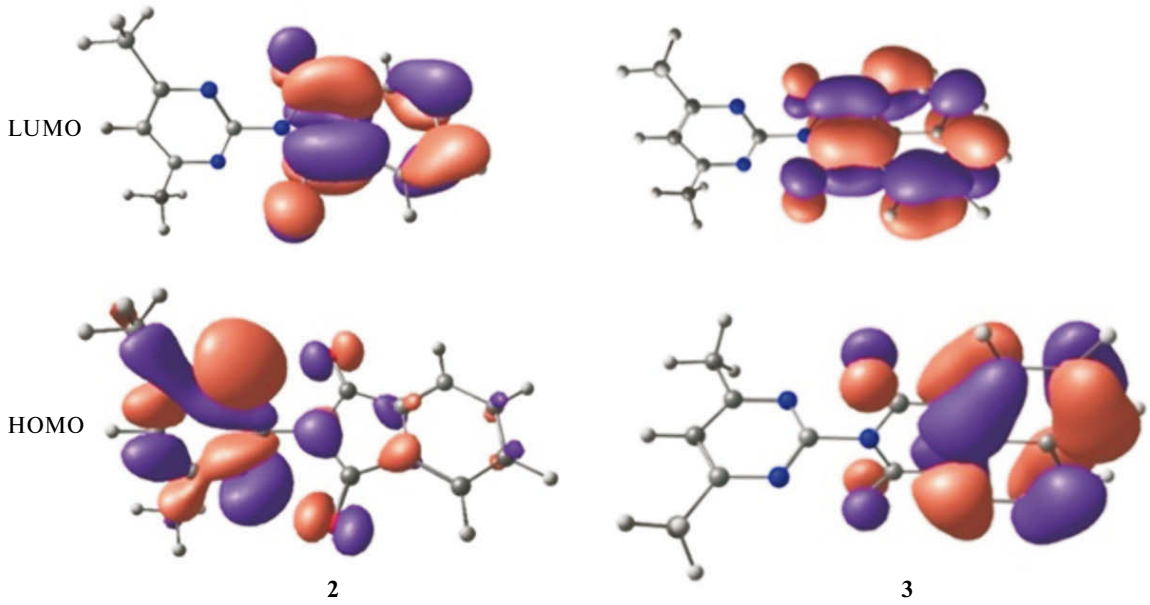

Fig. 8. Electron density distribution in the molecules of compounds **2** and **3**.

LUMO energies are typical for materials with electron conductivity.[37]

The geometric and electronic structures of the synthesized compounds were studied in the gas phase by quantum chemical calculations at the PBE0-D3/Def2-TZVPD level of theory using the Firefly program[38] partially based on the original GAMESS (US) source code.[39] The calculations showed that the electron density of HOMO and LUMO in compound **2** is located on the pyrimidine and phthalimide rings, respectively. In pyrimidine **3**, the HOMO electron density is concentrated in the naphthalene ring of the 1,8-naphthalimide moiety; the LUMO electron density — in the 1,8-naphthalimide moiety (Fig. 8).

The calculated HOMO energies of chromophores **3—11** are in good agreements with the corresponding experimental characteristics (see Table 1), whereas the calculated LUMO energies significantly differ from the parameters determined from electrochemical measurements. We believe that the most reasonable prediction of the band gap width between HOMO and LUMO can be made based on calculations of the vertical transition energy from the ground state S_0 to the excited state S_1 (the vertical excitation energy, S_0—S_1). This way of determination of the band gap width is more physically meaningful compared to calculations directly from the energy difference between the HOMO and LUMO eigenvalues.[40]

The HOMO electron density in compounds **4—11** is located on the π-conjugated system composed of 2-aryl-(hetaryl)vinyl moieties and the C(4), C(5), and C(6) atoms of the pyrimidine ring (Fig. 9). In compound **7**, the LUMO electron density is completely located on the phthalimide moiety. In compound **5**, the LUMO electron density is concentrated also at the nitrogen atoms of the pyrimidine ring and the vinyl carbon atoms directly bonded to this ring. In compounds **4** and **6**, the LUMO electron density is distributed along the conjugation chain and is present also on the terminal *p*-tolyl (**4**) and thiophene (**6**) moieties. In compounds **8—11**, the LUMO electron density is completely concentrated on the 1,8-naphthalimide moieties of the molecules (see Fig. 9).

The optical properties of pyrimidines **2—11** were studied by UV and fluorescence spectroscopy (Figs 10—13). The optical characteristics of substituted phthalimides **4—7** and substituted 1,8-naphthalimides **8—11** vary depending on the nature of the aryl or hetaryl moiety. Compounds **4—11** absorb in the region from 310 to 505 nm, which corresponds to the intramolecular charge transfer from the electron-donating hetaryl moiety to the electron-withdrawing core (see Figs 10 and 12). The absorption band maxima of chromophores **5** and **9** and also of **7** and **11** containing the *N*-hexylcarbazole and *N*-methylpyrrole moieties, respectively, undergo a bathochromic shift with respect to the absorption band maxima in the spectra of *p*-tolyl- and thiophene-containing chromophores **4**, **6**, **8**, and **10**. The emission spectra (see Figs 11 and 13) show that chromophores **4** and **6** and also **8** and **10** exhibit fluorescence in the blue region, whereas chromophores **5** and **9** and also **7** and **11** show fluorescence in the yellow region.

The relative fluorescence quantum yield increases in the series of compounds **4—7** bearing the phthalimide moiety in the order **6** < **7** < **4** < **5**; the same pattern is observed for the compounds containing the 1,8-naphthalimide moiety (**10** < **11** < **8** < **9**). The highest molar absorption coefficients (ε) are observed for solutions of the compounds containing the carbazole moiety

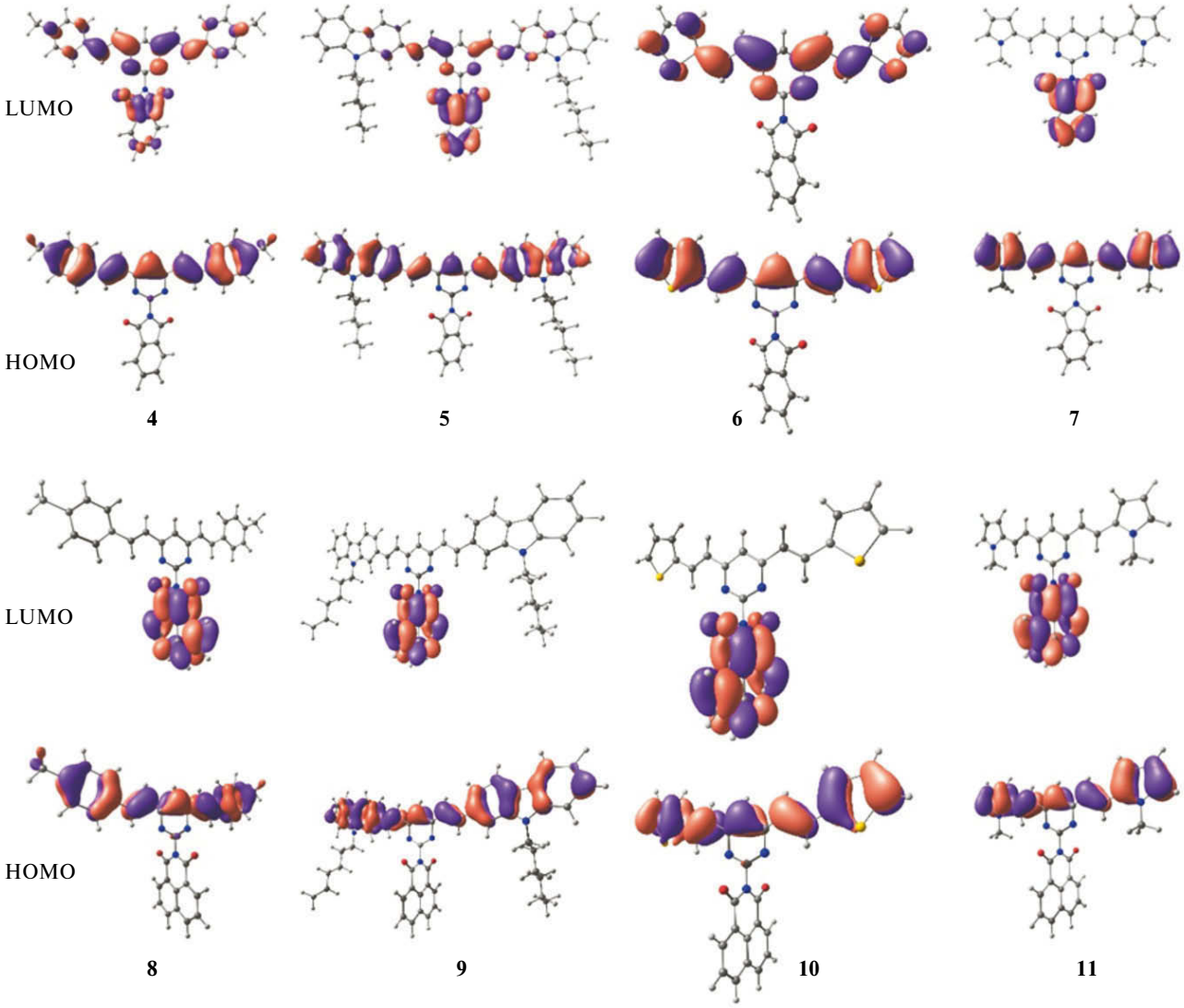

Fig. 9. Electron density distribution in the HOMO and LUMO in the molecules of compounds **4—11**.

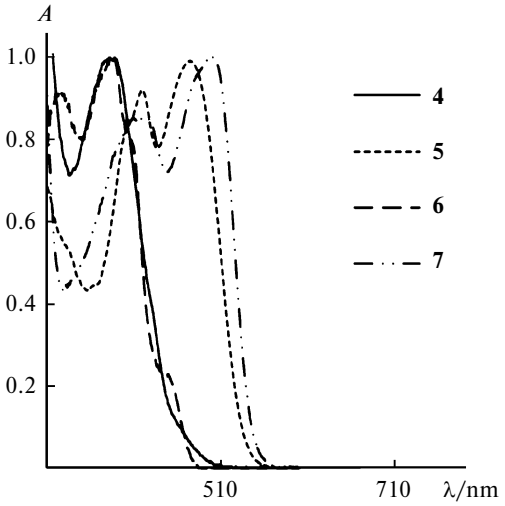

Fig. 10. Electronic absorption spectra of solutions of compounds **4—7** in THF ($C = 1 \cdot 10^{-5}$ mol L^{-1}).

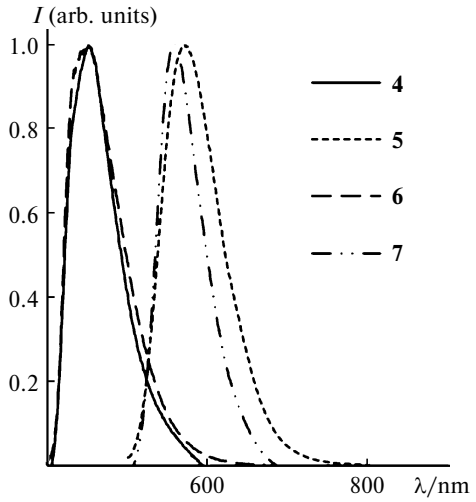

Fig. 11. Emission spectra of solutions of compounds **4—7** in THF ($C = 1 \cdot 10^{-6}$ mol L^{-1}) at λ_{ex} of 380 (**4**, **6**), 500 (**5**), and 430 nm (**7**).

Table 2. Optical characteristics of compounds **2—11**

Compound	λ_{max}^{abs}/nm (ε/L mol^{-1} cm^{-1})	λ_{max}^{em}	λ_{onset}	E_g^{abs}/eV	Δν/cm^{-1}	Φ_F
		nm				
2	290 (11150)	473	390	3.17	—	0.097[a]
3	330 (15870), 340 (14280)	372	375	3.31	2530	0.048[b]
4	312 (17860), 375 (18850)	454	480	2.58	4640	0.35[a]
5	420 (36900), 475 (34450)	570	555	2.23	3509	0.43[c]
6	325 (16481), 387 (16219)	450	482	2.57	4446	0.08[a]
7	408 (24200), 500 (22350)	560	556	2.23	2143	0.21[d]
8	320 (29250), 348 (26050), 375 (22550)	450	480	2.58	4444	0.36[a]
9	374 (39500), 471 (41300)	567	526	2.35	3595	0.39[c]
10	325 (18210), 389 (19030)	448	480	2.58	3385	0.12[a]
11	310 (8650), 505 (28300)	560	563	2.20	1944	0.20[d]

Notes: λ_{max}^{abs} is the absorption band maximum, ε is the molar absorption coefficient, λ_{onset} is the onset absorption wavelength in the red region, λ_{max}^{em} is the emission band maximum, E_g^{abs} is the optical band gap calculated by the formula $1240/\lambda_{onset}$, Δν is the Stokes shift (cm^{-1}) calculated by the formula $10^7(1/\lambda_{max}^{abs} - 1/\lambda_{max}^{em})$, Φ_F is the fluorescence quantum yield, which was determined using the following compounds as the standard: for compounds **2**, **4**, **8**, and **10**, aminophthalimide in EtOH ($\Phi_F = 0.6$, $\lambda_{ex} = 380$ nm);[43] for compound **3**, quinine sulfate in 0.1 N H_2SO_4 ($\Phi = 0.55$, $\lambda_{ex} = 340$ nm);[44] for compounds **5** and **9**, rhodamine B in EtOH ($\Phi_F = 0.65$, $\lambda_{ex} = 500$ nm);[45] for compounds **7** and **11**, rhodamine B in EtOH ($\Phi_F = 0.65$, $\lambda_{ex} = 490$ nm).[45]

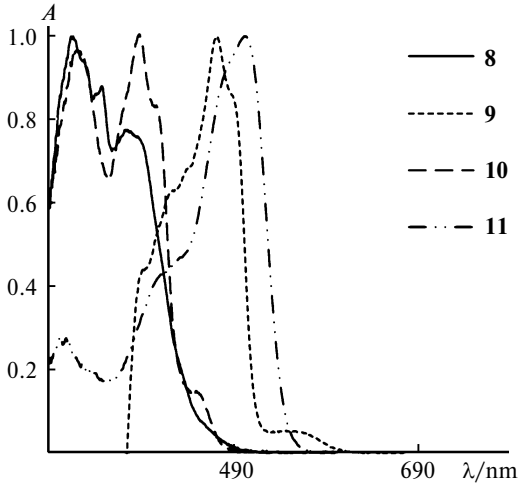

Fig. 12. Electronic absorption spectra of solutions of compounds **8—11** in THF ($C = 1 \cdot 10^{-5}$ mol L^{-1}).

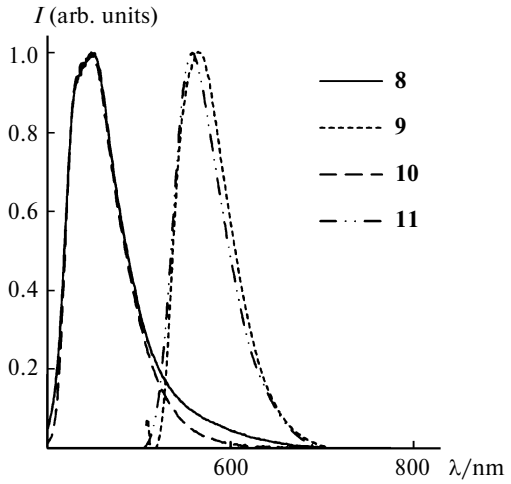

Fig. 13. Emission spectra of solutions of compounds **8—11** in THF ($C = 1 \cdot 10^{-6}$ mol L^{-1}) at λ_{ex} of 380 (**8**, **10**), 400 (**9**), and 505 nm (**11**).

(34450 L mol^{-1} cm^{-1} for **5** and 41050 L mol^{-1} cm^{-1} for **9**). A comparison of the optical characteristics of the compounds bearing the same aryl(hetaryl) groups but different imide moieties demonstrates that their properties are very similar (Table 2), except for the starting compounds **2** and **3**.

Thin films on quartz plates were prepared from solutions of compounds **4—11** in chlorobenzene by the centrifugation (spin-coating technique) in an argon-filled Glovebox system. The spectroscopic characteristics of the films of pyrimidines confirm the patterns of changes in the optical properties, which were observed for solutions of these chromophores in THF (Table 3, Figs 14 and 15).

In summary, we synthesized and characterized two series of D—π-A—π-D chromophores, which consist of the electron deficient 2-(4,6-dimethylpyrimidin-2-yl)-phthalimide or 2-(4,6-dimethylpyrimidin-2-yl)-1,8-naphthalimide core linked to electron-donating aromatic carbo- or heterocyclic moieties by the vinyl bridge. The

Table 3. Optical characteristics of films of chromophores **4—11**

Compound	λ_{max}^{abs}	λ_{max}^{em}	λ_{onset}	E_g^{opt}/eV	Δν/cm^{-1}
	nm				
4	396	530	480	2.50	6385
5	416	610	600	2.07	7645
6	370	460	460	2.58	5333
7	405	606	602	2.06	8190
8	385	530	470	2.64	7107
9	410	600	580	2.14	7724
10	370	500	500	2.48	7027
11	430	660	560	2.21	8104

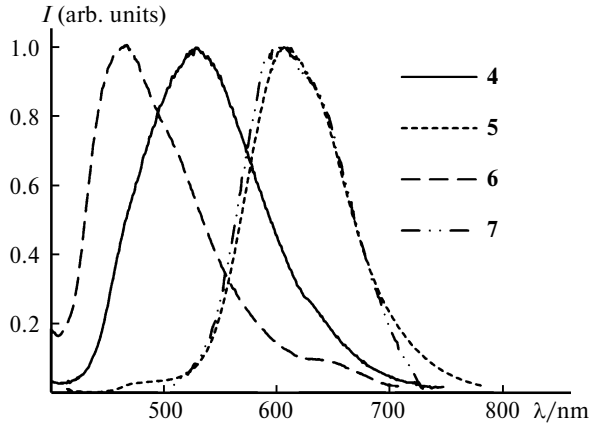

Fig. 14. Emission spectra of films of compounds **4—7**.

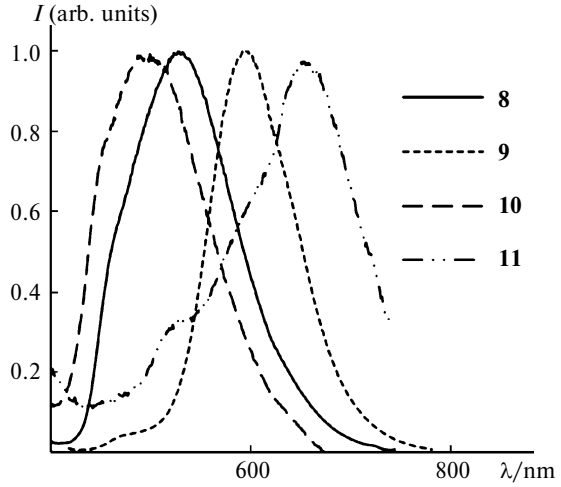

Fig. 15. Emission spectra of films of compounds **8—11**.

LUMO energy of 4,6-disubstituted pyrimidin-2-yl-1,8-naphthalimides varies in the range from −3.98 to −3.80 eV; for 4,6-disubstituted pyrimidin-2-ylphthalimides, the LUMO energy is from −4.38 to −4.23 eV. These compounds can be considered as semiconductors with electron conductivity. The presence of *N*-hexylcarbazole and *N*-methylpyrrole moieties in the chromophore structure leads to a red shift of the absorption and fluorescence maxima wavelengths in THF solutions and to the increase of the molar absorption coefficient and fluorescence quantum yield. The fluorescence maxima were found to strongly depend on the nature of the aryl(hetaryl) moiety. Thus, the thiophene-containing chromophores exhibit fluorescence in the blue region; the chromophores bearing *p*-tolyl moieties, in the green region; the chromophores containing strong electron-donating moieties (carbazole, *N*-methylpyrrole), in the orange region.

Experimental

The ^{1}H and ^{13}C NMR spectra were recorded on a Bruker AvanceNeo III HD spectrometer (400 MHz) with tetramethylsilane as the internal standard. The signals of protons are denoted as follows: pyrimidine ring, Pyrim; pyrrole ring, Pyr; thiophene ring, Th; carbazole moiety, Cz; phthalimide, PI; 1,8-naphthalimide, NPI. The IR spectra were measured on a SpectrumTwo FTIR spectrometer (Perkin-Elmer).

The X-ray diffraction data sets were collected at 295(2) K on an X-calibur 3 single-crystal X-ray diffractometer (Oxford Diffraction) using monochromatic Mo-Kα radiation (0.71073 Å) and a graphite monochromator. The structures were solved by direct methods with the SHELXS-90 program package (Sheldrick, 1990) and refined by the least-squares method with the SHELXL-97 program package (Sheldrick, 1997). The crystallographic data for compound **2**: $C_{14}H_{11}N_3O_2$, M = 253.26, triclinic, a = 8.2270(19) Å, b = 12.1529(18) Å, c = 14.282(2) Å, α = 110.285(14)°, β = 102.620(20)°, γ = 98.738(17)°, V = 1265.9(4) Å^3, T = 295(2), space group $P\bar{1}$, Z = 4, μ(Mo-Kα) = = 0.092 mm^{-1}. The final refinement parameters: R_1 = 0.0543, wR_2 = 0.1264 (for 3820 reflections with $I > 2\sigma(I)$); R_1 = 0.0890, wR_2 = 0.1530 (for a total of 5872 independent reflections, R_{int} = 0.0279), S = 1.027. The maximum and minimum residual electron density peaks are 0.189 and −0.242 e Å^{-3}, respectively. The crystallographic data for compound **3**: $C_{18}H_{13}N_3O_2$, M = 303.31, monoclinic, a = 14.360(3) Å, b = 13.458(3) Å, c = 16.107(4) Å, β = 110.21(3)°, V = 2921.1(13) Å^3, T = 295(2), space group $P2_1/c$, Z = 8, μ(Mo-Kα) = 0.093 mm^{-1}. The final refinement parameters: R_1 = 0.0593, wR_2 = 0.1347 (for 4111 reflections with $I > 2\sigma(I)$); R_1 = 0.1076, wR_2 = 0.1654 (for a total of 6988 independent reflections, R_{int} = 0.0295), S = 1.022. The maximum and minimum residual electron density peaks are 0.241 and −0.215 e Å^{-3}, respectively.

Elemental analysis was performed using a CHNS-932 LECO Corp analyzer. The melting points were determined with Mettler Toledo MP 70 and NETZSCH DSC 214 Polyma DSC21400A-0115-L apparatuses. Fluorescence spectra were recorded on a Shimadzu RF-5301pc spectrofluorometer. The cell size was 10×10 mm, the concentrations of solutions were 10^{-6}—10^{-5} mol L^{-1}. The relative quantum yields were calculated using a procedure described in the monograph[44] for three—five solutions of each compound at concentrations of 10^{-6}—10^{-7} mol L^{-1}. The UV spectra were recorded on a UV-2600 UV-VIS spectrometer (Shimadzu), the concentration of the solutions was 10^{-5} mol L^{-1}. The spectra were processed with the UV Probe 2.42 software and the Panorama 3.1 Fluorescence.

The course of the reactions was monitored and the purity of the compounds was checked by TLC on Sorbfil plates. The mixtures were separated and the target products were purified on a column packed with silica gel (Lancaster, silica gel 60, 0.060—0.2 mm) using eluents, which were chosen by means of TLC. Electrochemical studies were carried out on a Potentiostat/Galvanostat/ZRA Interface 1000 instrument in a conventional three-electrode cell using an ITO electrode (glass plates coated on their inwardly facing surfaces with a conductive indium—tin oxide layer, R_s = 8—12 Ohm, Aldrich) as the working electrode, platinum wire as the auxiliary electrode (ERL-02), the silver chloride reference electrode (EVL-1M4), ~20 °C. A 4 : 1 CH_3CN—CH_2Cl_2 mixture (10 mL) was used as the solvent; $(C_2H_5)_4N^+ClO_4^-$ was used as ClO_4^- the background electrolyte, $C_{background}$ = 0.1 mol L^{-1}, $C_{compound}$ = 1·10^{-3} mol L^{-1}; the potential scan rate was V_{scan} = 100 mV s^{-1}. The cyclic voltammetry data were processed with the Gammy Instruments Framework Date Acquisition Version 6.25; the curves were constructed using Microsoft Excel tools (2007, 2013). Quantum chemical

calculations were performed at the PBE0-D3/Def2-TZVPD level of theory in the gas phase with he Firefly program partially based on the original GAMESS (US) source code using a PSU-Kepler supercomputer.

The following commercial reagents were used: *p*-toluic aldehyde (AlfaAesar), thiophene-2-carbaldehyde (AlfaAesar), *N*-methylpyrrole-2-carbaldehyde (AlfaAesar), phthalic anhydride (AlfaAesar), and 1,8-naphthalic anhydride (AlfaAesar).

Synthesis of compounds 2 and 3 (general procedure).[46] A mixture of phthalic or naphthalic anhydride (7.3 mmol) and 2-amino-4,6-dimethylpyrimidine (8.1 mmol, 1 g) in dry DMF (10 mL) was refluxed under an argon atmosphere for 24 h until an orange-brown suspension formed. Then excess DMF was distilled off under reduced pressure. The residue was washed with hexane and dried in air. The product was purified by recrystallization from an appropriate solvent.

***N*-(4,6-Dimethylpyrimidin-2-yl)phthalimide (2).** Yellow crystalline compound. Yield 3.2 g (80%), m.p. 118—120 °C. Found (%): C, 66.51; H, 4.41; N, 16.04. $C_{14}H_{11}N_3O_2$. Calculated (%): C, 66.40; H, 4.38; N, 16.59. IR (Nujol mulls), ν/cm^{-1}: 3366, 1673, 1608, 1580, 1266. ^{1}H NMR ($CDCl_3$), δ: 2.57 (s, 6 H, 2 CH_3); 7.12 (s, 1 H, Pyrim); 7.79 q, 2 H, PI, J = 7.8 Hz); 7.93 (q, 2 H, PI, J = 7.9 Hz). ^{13}C NMR ($CDCl_3$), δ: 23.6, 119.6, 123.7, 131.6, 134.3, 152.7, 165.9, 169.2.

***N*-(4,6-Dimethylpyrimidin-2-yl)-1,8-naphthalimide (3).** Yellow crystalline compound. Yield 4.1 g (85%), m.p. 253—255 °C. Found (%): C, 70.97; H, 4.20; N, 13.18. $C_{18}H_{13}N_3O_2$. Calculated (%): C, 71.28; H, 4.32; N, 13.85. IR (Nujol mulls), ν/cm^{-1}: 3335, 1774, 1705, 1670, 1584, 1246. ^{1}H NMR ($CDCl_3$), δ: 2.59 (s, 6 H, 2 CH_3); 7.15 (s, 1 H, Pyrim); 7.74 (t, 2 H, NPI, J = 7.8 Hz); 8.23 (d, 2 H, NPI, J = 8.1 Hz); 8.59 (d, 2 H, NPI, J = 7.1 Hz). ^{13}C NMR ($CDCl_3$), δ: 23.8, 120.2, 122.7, 126.9, 127.4, 128.7, 131.4, 131.8, 133.3, 134.5, 135.3, 156.1, 163.9, 169.8.

Synthesis of compounds 4—11 (general procedure). A mixture of 4,6-dimethyl-2-substituted pyrimidine **2** or **3** (0.1 mmol) and appropriate carbaldehyde (0.2 mmol) was refluxed for 5 h under an argon atmosphere in a 5 *M* aqueous NaOH solution in the presence of a catalytic amount of Aliquat 336. Then the solution was cooled to ~20 °C, poured into water, and extracted with CH_2Cl_2. The combined organic extracts were washed with water and dried over Na_2SO_4. Excess solvent was distilled off, and the residue was dried in air. Compounds **4—11** were isolated and purified by silica gel column chromatography (CH_2Cl_2).

***N*-{4,6-Bis[(*E*)-2-(4-methylphenyl)ethenyl]pyrimidin-2-yl}-phthalimide (4).** Yellow crystalline compound. Yield 40 mg (85%), m.p. 132.5 °C. Found (%): C, 78.31; H, 4.94; N, 8.63. $C_{30}H_{23}N_3O_2$. Calculated (%): C, 78.75; H, 5.07; N, 9.18. ^{1}H NMR ($CDCl_3$), δ: 2.41 (s, 6 H, 2 CH_3); 6.76 (s, 1 H, Pyrim); 6.93 (d, 2 H, 2 CH=, J = 15.9 Hz); 7.23 (d, 4 H, C_6H_4, J = 8.0 Hz); 7.61—7.44 (m, 8 H, C_6H_4, PI); 7.83 (d, 2 H, 2 CH=, J = 16.0 Hz). ^{13}C NMR ($CDCl_3$), δ: 21.3, 107.4, 109.0, 125.5, 127.6, 129.6, 133.3, 136.8, 139.5, 163.2, 164.1, 169.2 (overlapping of signals).

***N*-{4,6-Bis[(*E*)-2-(9-hexyl-9*H*-carbazol-3-yl)ethenyl]pyrimidin-2-yl}phthalimide (5).** Red crystalline compound. Yield 60 mg (79%), m.p. 80.6 °C. Found (%): C, 80.01; H, 6.24; N, 8.66. $C_{52}H_{49}N_5O_2$. Calculated (%): C, 80.49; H, 6.36; N, 9.03. ^{1}H NMR ($CDCl_3$), δ: 0.86 (t, 6 H, 2 $NCH_2CH_2CH_2CH_2CH_2C\underline{H}_3$, J = 7.0 Hz); 1.39—1.28 (m, 12 H, 2 $NCH_2CH_2C\underline{H}_2C\underline{H}_2C\underline{H}_2CH_3$); 1.87 (m, 4 H, 2 $NCH_2C\underline{H}_2CH_2CH_2CH_2CH_3$); 4.28 (t, 4 H, 2 N—$CH_2$, J = 7.3 Hz); 6.74 (s, 1 H, Pyrim); 6.91 (d, 2 H, 2 CH=, J = 15.8 Hz); 7.29—7.26 (m, 6 H, Cz); 7.40 (d, 4 H, Cz, J = 8.3 Hz); 7.48 (t, 2 H, Cz, J_1 = 7.9 Hz, J_2 = 7.3 Hz); 7.77 (d, 2 H, PI, J = 8.4 Hz); 8.13 (d, 2 H, PI, J = 7.6 Hz); 8.35 (m, 4 H, Cz, 2 CH=). ^{13}C NMR ($CDCl_3$), δ: 13.9, 22.5, 26.9, 28.9, 31.5, 43.3, 107.3, 109.0, 119.3, 120.2, 120.5, 122.9, 123.3, 123.6, 125.4, 126.0, 127.2, 137.3, 140.9, 141.1, 163.0, 164.3 (overlapping of signals).

***N*-{4,6-Bis[(*E*)-2-(thiophen-2-yl)ethenyl]pyrimidin-2-yl}-phthalimide (6).** Yellow crystalline compound. Yield 30 mg (75%), m.p. 142.3 °C. Found (%): C, 64.98; H, 3.30; N, 9.01; S, 14.27. $C_{24}H_{15}N_3O_2S_2$. Calculated (%): C, 65.29; H, 3.42; N, 9.52; S, 14.52. ^{1}H NMR ($CDCl_3$), δ: 6.60 (s, 1 H, Pyrim); 6.65 (d, 2 H, 2 CH=, J = 15.8 Hz); 7.09 (d, 2 H, Th, J = 5.0 Hz); 7.29 (d, 2 H, Th, J = 2.5 Hz); 7.35 (d, 2 H, Th, J = 4.9 Hz); 7.40 (d, 2 H, PI, J = 5.4 Hz); 7.44 (d, 2 H, PI, J = 5.1 Hz); 8.12 (d, 2 H, 2 CH=, J = 15.5 Hz). ^{13}C NMR ($CDCl_3$), δ: 107.9, 125.6, 126.6, 127.5, 127.9, 128.8, 129.5, 133.3, 136.1, 139.2, 141.5, 163.6.

***N*-{4,6-Bis[(*E*)-2-(1-methyl-1*H*-pyrrol-2-yl)ethenyl]pyrimidin-2-yl}phthalimide (7).** Red crystalline compound. Yield 30 mg (72%), m.p. 195 °C. Found (%): C, 71.40; H, 4.59; N, 15.71. $C_{26}H_{21}N_5O_2$. Calculated (%): C, 71.71; H, 4.86; N, 16.08. ^{1}H NMR ($CDCl_3$), δ: 3.89 (s, 6 H, 2 N—CH_3); 6.28 (q, 2 H, Pyr, J = 3.8 Hz); 6.32 (s, 1 H, Pyrim); 6.44 (d, 2 H, 2 CH=, J = 15.5 Hz); 6.88 —6.91 (m, 4 H, Pyr); 7.80 (m, 4 H, PI); 8.45 (d, 2 H, 2 CH=, J = 15.4 Hz). ^{13}C NMR ($CDCl_3$), δ: 34.3, 68.2, 107.9, 108.2, 108.6, 109.0, 109.1, 109.7, 109.9, 112.4, 125.1, 125.4, 125.6, 128.8, 130.8, 131.1.

***N*-{4,6-Bis[(*E*)-2-(4-methylphenyl)ethenyl]pyrimidin-2-yl}-1,8-naphthalimide (8).** Yellow crystalline compound. Yield 40 mg (83%), m.p. 109 °C. Found (%): C, 80.05; H, 4.84; N, 7.76. $C_{34}H_{25}N_3O_2$. Calculated (%): C, 80.45; H, 4.96; N, 8.28. ^{1}H NMR ($CDCl_3$), δ: 2.37 (s, 6 H, 2 CH_3); 6.71 (s, 1 H, Pyrim); 6.87 (d, 2 H, 2 CH=, J = 16.0 Hz); 7.18 (d, 4 H, C_6H_4, J = 7.8 Hz); 7.48 (d, 4 H, C_6H_4, J = 7.9 Hz); 7.75 (t, 2 H, NPI, J_1 = 7.4 Hz, J_2 = 8.1 Hz); 7.89 (d, 2 H, 2 CH=, J = 16.0 Hz); 8.3 (dd, 2 H, NPI, J_1 = 8.3 Hz, J_2 = 8.4 Hz); 8.61 (dd, 2 H, NPI, J_1 = 7.4 Hz, J_2 = 7.3 Hz). ^{13}C NMR ($CDCl_3$), δ: 21.4, 107.3, 120.1, 122.9, 126.6, 126.9, 128.0, 129.7, 131.4, 132.8, 134.4, 139.1, 156.1, 140.3, 163.9, 168.9.

***N*-{4,6-Bis[(*E*)-2-(9-hexyl-9*H*-carbazol-3-yl)ethenyl]pyrimidin-2-yl}-1,8-naphthalimide (9).** Red crystalline compound. Yield 60 mg (73%), m.p. (decomp.) ~ 200 °C. Found (%): C, 81.12; H, 6.25; N, 7.86. $C_{56}H_{51}N_5O_2$. Calculated (%): C, 81.42; H, 6.22; N, 8.48. ^{1}H NMR ($CDCl_3$), δ: 0.86 (t, 6 H, 2 $NCH_2CH_2CH_2CH_2CH_2C\underline{H}_3$, J = 7.0 Hz); 1.39—1.28 (m, 12 H, 2 $NCH_2CH_2C\underline{H}_2C\underline{H}_2C\underline{H}_2CH_3$); 1.87 (m, 4 H, 2 $NCH_2C\underline{H}_2CH_2CH_2CH_2CH_3$); 4.27 (t, 4 H, 2 N—$CH_2$, J = 7.1 Hz); 6.76 (s, 1 H, Pyrim); 6.93 (d, 2 H, 2 CH=, J = 15.9 Hz); 7.26—7.48 (m, 10 H, Cz); 7.74 (t, 2 H, NPI, J = 7.5 Hz); 8.10—8.17 (m, 4 H, 2 CH=, NPI); 8.22 (d, 2 H, NPI, J = 8.3 Hz); 8.31 (s, 2 H, Cz); 8.60 (d, 2 H, NPI, J = 7.3 Hz). ^{13}C NMR ($CDCl_3$), δ: 13.4, 22.5, 26.9, 28.9, 31.5, 43.4, 106.8, 107.2, 108.9, 109.1, 109.2, 119.6, 120.6, 121.0, 122.8, 123.0, 123.6, 125.9, 126.3, 126.6, 126.9, 127.5, 131.4, 134.4, 136.9, 141.1, 141.7, 168.5.

***N*-{4,6-Bis[(*E*)-2-(thiophen-2-yl)ethenyl]pyrimidin-2-yl}-1,8-naphthalimide (10).** Yellow crystalline compound. Yield 30 mg (68%), m.p. 193 °C. Found (%): C, 68.24; H, 3.37; N, 7.98; S, 12.57. $C_{28}H_{17}N_3O_2S_2$. Calculated (%): C, 68.41; H, 3.49; N, 8.55; S, 13.05. ^{1}H NMR ($CDCl_3$), δ: 6.65 (s, 1 H, Pyrim); 6.77 (d, 2 H, 2 CH=, J = 15.6 Hz); 7.06 (d, 2 H, Th, J = 3.6 Hz); 7.23 (d, 2 H, Th, J = 3.5 Hz); 7.32 (d, 2 H, Th, J = 5.0 Hz); 7.53 (d, 2 H, NPI, J = 5.6 Hz); 7.73 (dd, 4 H, NPI, J = 5.6 Hz); 7.92 (d, 2 H, 2 CH=, J = 15.6 Hz). ^{13}C NMR ($CDCl_3$), δ: 108.0, 125.6, 126.7, 127.9, 128.8, 129.0, 130.8, 132.6, 141.6, 163.0, 163.7, 167.6 (overlapping of signals).

***N*-{4,6-Bis[(*E*)-2-(1-methyl-1*H*-pyrrol-2-yl)ethenyl]pyrimidin-2-yl}-1,8-naphthalimide (11).** Red crystalline compound. Yield 30 mg (69%), m.p. (decomp.) ~187 °C. Found (%): C, 74.30; H, 4.60; N, 13.84. $C_{30}H_{23}N_5O_2$. Calculated (%): C, 74.21; H, 4.77; N, 14.42. ^{1}H NMR ($CDCl_3$), δ: 3.77 (s, 6 H, 2 N—CH_3); 6.18 (m, 2 H, Pyr); 6.45 (s, 1 H, Pyrim); 6.56—6.73 (m, 6 H, Pyr, 2 CH=); 7.50 (m, 2 H, NPI); 7.68 (m, 2 H, NPI); 7.86 (d, 2 H, 2 CH=, J = 15.8 Hz); 8.57 (d, 2 H, NPI, J = 7.3 Hz). ^{13}C NMR ($CDCl_3$), δ: 34.4, 68.2, 107.6, 109.6, 121.8, 122.7, 125.6, 127.4, 128.8, 130.8, 132.6, 156.6, 164.5, 170.1 (overlapping of signals).

This work was financially supported by the Russian Foundation for Basic Research (Project No. 18-33-00323 mol_a).

References

1. J.-P. Malval, S. Achelle, L. Bodiou, A. Spangenberg, L. C. Gomez, O. Soppera, F. R. Guen, *J. Mater. Chem. C*, 2014, **2**, 7869.
2. S. S. Gunathilake, P. Huang, M. P. Bhatt, E. A. Rainbolt, M. C. Stefan, M. C. Biewer, *RSC Adv.*, 2014, **4**, 41997.
3. S. Achelle, J. Rodríguez-López, F. R. Guen, *Chem. Select.*, 2018, **3**, 1852.
4. K. Nakao, H. Sasabe, R. Komatsu, Y. Hayasaka, T. Ohsawa, J. Kido, *Adv. Optical Mater.*, 2017, 1600843.
5. E. V. Verbitskiy, E. M. Dinastiya, A. A. Baranova, K. O. Khokhlov, R. D. Chuvashov, Y. A. Yakovleva, N. I. Makarova, E. V. Vetrova, A. V. Metelitsa, P. A. Slepukhin, G. L. Rusinov, O. N. Chupakhin, V. N. Charushin, *Dyes Pigm.*, 2018, **159**, 35.
6. E. V. Verbitskiy, A. A. Baranova, K. I. Lugovik, K. O. Khokhlov, E. M. Cheprekova, G. L. Rusinov, O. N. Chupakhin, V. N. Charushin, *Arkivoc*, 2016, 360.
7. S. Achelle, I. Nouira, B. Pfaffinger, Y. Ramondenc, N. Plé, J. Rodríguez-López, *J. Org. Chem.*, 2009, **74**, 3711.
8. S. Kato, Y. Yamada, H. Hiyoshi, K. Umezu, Y. J. Nakamura, *J. Org. Chem.*, 2015, **80**, 9076.
9. S. Achelle, J. Rodríguez-López, N. Cabon, F. R. Guen, *RSC Adv.*, 2015, **5**, 107396.
10. R. Komatsu, H. Sasabe, J. Kido, *J. Photon. Energy*, 2018, **8**, 032108.
11. M. Klikar, P. le Poul, A. Rüzička, O. Pytela, A. Barsella, K. D. Dorkenoo, F. Robin-le Guen, F. Bureš, S. Achelle, *J. Org. Chem.*, 2017, **82**, 9435.
12. T. Kojima, J. Nishida, S. Tokito, Y. Yamashita, *Chem. Lett.*, 2009, **38**, 428.
13. R. P. Ortiz, H. Yan, A. Facchetti, T. J. Marks, *Materials*, 2010, **3**, 1533.
14. J. Kim, J. Lee, S. Chae, J. Y. Shim, D. Y. Lee, L. Kim, H. J. Kim, S. H. Park, H. Suh, *Polymer*, 2016, **83**, 50.
15. D. Vulpeş, A. Chiriac, *Ann. W.U.T-Ser. Chem.*, 2009, **18**, 53.
16. X. Mamtimin, A. Aikebaierjiang, M. Alifujiang, T. Tuerxun, Z. Kurban, W. F. Sun, I. Nurulla, *J. Polym. Res.*, 2011, **18**, 105.
17. V. Theodorou, M. Gogou, A. Giannousi, K.Skobridis, *Arkivoc*, 2014, 11.
18. C. Wang, H. Dong, W. Hu, Y. Liu, D. Zhu, *Chem. Rev.*, 2012, **112**, 2208.
19. Z. H. Wu, Z. T. Huang, R. X. Guo, C. L. Sun, L. C. Chen, B. Sun, Z. F. Shi, X. Shao, H. Li, H.-L. Zhang, *Angew. Chem., Int. Ed. Engl.*, 2017, **56**, 13031.
20. F.-P. Wu, H. Un, Y. Li, H. Hu, Y. Yuan, B. Yang, K. Xiao, W. Chen, J.-Y. Wang, Z.-Q. Jiang, J. Pei, L.-S. Liao, *Chem. Eur. J.*, 2017, **23**, 14723.
21. S. Ge, B. Li, X. Meng, H. Yan, M. Yang, B. Dong, Y. Lu, *Dyes Pigm.*, 2018, **148**, 147.
22. J.-Z. Liao, X.-Y. Wu, J.-P. Yong, H.-L. Zhang, W.-B. Yang, R. Yu, C.-Z. Lu, *Cryst. Growth Des.*, 2015, **15**, 4952.
23. W. Zhu, M. Hu, R. Yao, H. Tian, *J. Photochem. Photobiol. A*, 2003, **154**, 169.
24. H. Cao, V. Chang, R. Hernandez, M. D. Heagy, *J. Org. Chem.*, 2005, **70**, 4929.
25. M. Li, Y. Liu, R. Duan, X. Wei, Y. Yi, Y. Wang, C.-F. Chen, *Angew. Chem., Int. Ed. Engl.*, 2017, **56**, 8818.
26. H. Yan, X. Meng, B. Li, S. Ge, Y. Lu, *J. Mater. Chem. C*, 2017, **5**, 10589.
27. M. Daskeviciene, S. Urnikaite, G. Planciunaite, T. Malinauskas, A. Gruodis, M. Viliunas, E. Kamarauskas, V. Gaidelis, V. Jankauskas, V. Getautis, *Dyes Pigm.*, 2018, **158**, 157.
28. Y. Qu, L. Wang, J. Wu, Y. Rui, J. Cao, J. Xu, *Dyes Pigm.*, 2018, **148**, 99.
29. G. Abashev, E. Sosnin, E. Shklyaeva, T. Ustalova, I. Osorgina, V. Romanova, *Phys. Status Solidi C*, 2012, **9**, 1127.
30. E. A. Komissarova, I. V. Lunegov, E. V. Shklyaeva, G. G. Abashev, *Chem. Heterocycl. Compd.*, 2016, **52**, 257.
31. E. A. Komissarova, E. Sosnin, E. V. Shklyaeva, I. V. Osorgina, G. G. Abashev, *Arkivoc*, 2017, 105.
32. E. A. Komissarova, M. V. Dmitriev, I. G. Mokrushin, A. N. Vasyanin, I. V. Lunegov, E. V. Shklyaeva, G. G. Abashev, *Mendeleev Commun.*, 2019, **29**, 47.
33. T. F. Scholz, N. J. Somerville, G. M. Smith, US Pat. 2660579, 1953; *Chem. Abstrs.*, 1954, **48**, 12184.
34. G. Sathiyan, R. Thangamuthu, P. Sakthivel, *RSC Adv.*, 2016, **6**, 69196.
35. J. J. Van den Eynde, L. Pascal, Y. Van Haverbeke, P. Dubois, *Synth. Commun.*, 2001, **31**, 3167.
36. C. F. Macrae, I. J. Bruno, J. A. Chisholm, P. R. Edgington, P. McCabe, E. Pidcock, L. Rodriguez-Monge, R. Taylor, J. van de Streek, P. A. Wood, *J. Appl. Crystallogr.*, 2008, **41**, 466.
37. X. Gao, Y. Hu, *J. Mater. Chem. C*, 2014, **2**, 3099.
38. A. A. Granovsky, *Firefly Version 8*, http://classic.chem.msu.su/gran/firefly/index.html.
39. M. W. Schmidt, K. K. Baldridge, J. A. Boatz, S. T. Elbert, M. S. Gordon, J. H. Jensen, S. Koseki, N. Matsunaga, K. A. Nguyen, S. Su, T. L. Windus, M. Dupuis, J. A. Montgomery, Jr, *J. Comput. Chem.*, 1993, **14**, 1347.
40. G. Zhang, C. B. Musgrave, *J. Phys. Chem.*, 2007, **111**, 1554.
41. J. Pommerehne, H. Vestweber, W. Guss, R. F. Mahrt, H. Bässler, M. Porsh, J. Daub, *Adv. Mater.*, 1995, **7**, 551.
42. C. M. Cardona, W. Li, A. E. Kaifer, D. Stockdale, G. C. Bazan, *Adv. Mater.*, 2011, **23**, 2367.
43. W. H. Melhuish, *J. Res. Natl. Bur. Stand.*, 1972, **76**, 547.
44. C. Parker, *Photoluminescence of Solutions with Applications to Photochemistry and Analytical Chemistry*, Elsevier, Amsterdam—London—New York, 1968, 544 pp.
45. R. F. Kubin, A. N. Fletcher, *J. Luminescence*, 1982, **27**, 455.
46. S. Guha, F. S. Goodson, L. J. Corson, S. Saha, *J. Am. Chem. Soc.*, 2012, **134**, 13679.

Received March 26, 2019;
in revised form May 28, 2019;
accepted June 20, 2019